Cell, Vol. 118, 477–491, August 20, 2004, Copyright ©2004 by Cell Press

Mouse Development and Cell Proliferation in the Absence of D-Cyclins

Katarzyna Kozar,[1,6] Maria A. Ciemerych,[1,7] Vivienne I. Rebel,[1] Hirokazu Shigematsu,[2] Agnieszka Zagozdzon,[1] Ewa Sicinska,[1,3] Yan Geng,[1] Qunyan Yu,[1] Shoumo Bhattacharya,[4] Roderick T. Bronson,[5] Koichi Akashi,[2] and Piotr Sicinski[1,*]

[1]Department of Cancer Biology
[2]Department of Cancer Immunology and AIDS
Dana-Farber Cancer Institute and Department of Pathology
Harvard Medical School
Boston, Massachusetts 02115
[3]Department of Pathology
Brigham and Women's Hospital
Harvard Medical School
Boston, Massachusetts 02115
[4]Department of Cardiovascular Medicine
University of Oxford
Oxford OX3 7BN
United Kingdom
[5]Tufts University School of Veterinary Medicine
North Grafton, Massachusetts 01536

Summary

D-type cyclins (cyclins D1, D2, and D3) are regarded as essential links between cell environment and the core cell cycle machinery. We tested the requirement for D-cyclins in mouse development and in proliferation by generating mice lacking all D-cyclins. We found that these cyclin D1$^{-/-}$D2$^{-/-}$D3$^{-/-}$ mice develop until mid/late gestation and die due to heart abnormalities combined with a severe anemia. Our analyses revealed that the D-cyclins are critically required for the expansion of hematopoietic stem cells. In contrast, cyclin D-deficient fibroblasts proliferate nearly normally but show increased requirement for mitogenic stimulation in cell cycle re-entry. We found that the proliferation of cyclin D1$^{-/-}$D2$^{-/-}$D3$^{-/-}$ cells is resistant to the inhibition by p16^{INK4a}, but it critically depends on CDK2. Lastly, we found that cells lacking D-cyclins display reduced susceptibility to the oncogenic transformation. Our results reveal the presence of alternative mechanisms that allow cell cycle progression in a cyclin D-independent fashion.

Introduction

The proliferation of mammalian cells is governed by cyclins and their associated cyclin-dependent kinases (CDKs). Cyclins represent regulatory subunits that bind, activate, and provide substrate specificity for their catalytic partners, CDKs. These cyclin-CDK complexes phosphorylate critical cellular substrates, thereby allowing cell cycle progression (Sherr and Roberts, 1999).

Among all cyclin classes, the family of D-type cyclins (cyclins D1, D2, and D3) stands out as a very unique component of the cell cycle apparatus. Unlike other cyclins that fluctuate periodically during cell cycle progression, the levels of D-cyclins are controlled by the extracellular environment. Thus, D-cyclins are induced by the mitogenic stimulation, and their levels decline when the mitogens are withdrawn (Sherr and Roberts, 1999). Once induced, D-cyclins associate with partner cyclin-dependent kinases CDK4 and CDK6. These cyclin D-CDK complexes phosphorylate the retinoblastoma tumor suppressor protein, pRB, as well as pRB-related proteins p107 and p130 (Sherr and Roberts, 1999). The "preparatory" phosphorylation of pRB by cyclin D-CDK4/6 is believed to represent a molecular switch that allows further phosphorylation by cyclin E-CDK2 and cyclin A-CDK2 complexes, leading to full pRB inactivation (Harbour et al., 1999; Lundberg and Weinberg, 1998). This, in turn, results in release or derepression of the E2F transcription factors and drives cell entry into the S phase (Dyson, 1998).

Moreover, the induction of cyclin D-CDK complexes causes redistribution of the cell cycle inhibitors p27^{Kip1} and p21^{Cip1} from cyclin E-CDK2 and cyclin A-CDK2 complexes (which are inhibited by p27^{Kip1} and p21^{Cip1}) to cyclin D-CDK complexes (which use these inhibitors as assembly factors), thereby triggering kinase activities associated with cyclins E and A (Sherr and Roberts, 1999). This represents yet another mechanism that subjects the core cell cycle machinery to control by the extracellular mitogenic stimulation, via D-cyclins.

Hence, according to our current understanding, the D-type cyclins appeared during the evolution to link the extracellular mitogenic stimulation with the core cell cycle machinery. Importantly, most of the studies suggested that at least one D-cyclin is required to allow mammalian cell proliferation. The work described below challenges this notion and reveals that our understanding of the core cell cycle machinery needs to be reevaluated.

Results

Embryonal Development in the Absence of D-Cyclins

In order to rigorously test the requirement for D-type cyclins in development and in cell proliferation, we intercrossed cyclin D1-, D2-, and D3-deficient animals in an attempt to produce conceptuses lacking all D-cyclins.

Very unexpectedly, we observed that embryos lacking all three D-cyclins can develop normally as late as at embryonal day 13.5 (E13.5), i.e., at a stage when most of the tissues and organs are already formed (Figure 1A). At E15.5, a significant fraction of cyclin D1$^{-/-}$D2$^{-/-}$D3$^{-/-}$ embryos remained viable, but the mutant embryos ap-

*Correspondence: peter_sicinski@dfci.harvard.edu
[6]Present address: Department of Immunology, Center of Biostructure Research, The Medical University of Warsaw, 02-004 Warsaw, Poland.
[7]Present address: Department of Embryology, Institute of Zoology, University of Warsaw, 02-096 Warsaw, Poland.

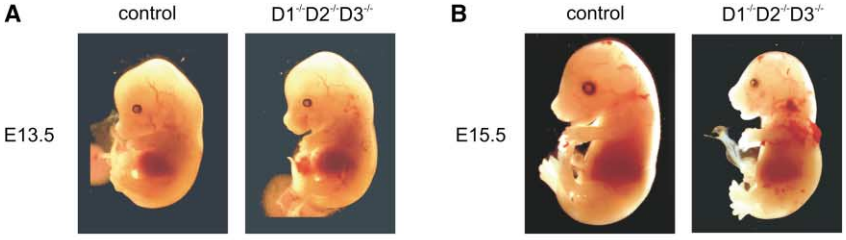

C

Day	Observed ratio	Expected ratio
E10.5	3/52	3/52
E13.5	14(1)/269	17/269
E14.5	21(12)/640	40/640
E15.5	5(11)/276	17/276
E16.5	1(5)/112	7/112
E17.5	(2)/39	2/39

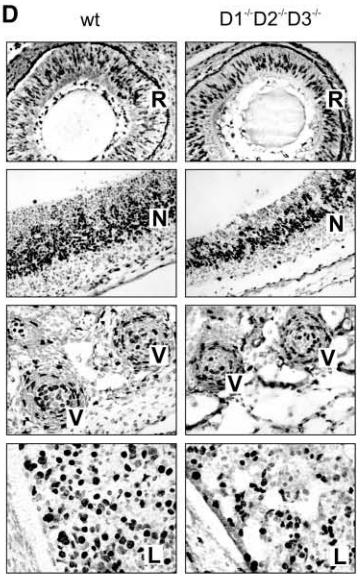

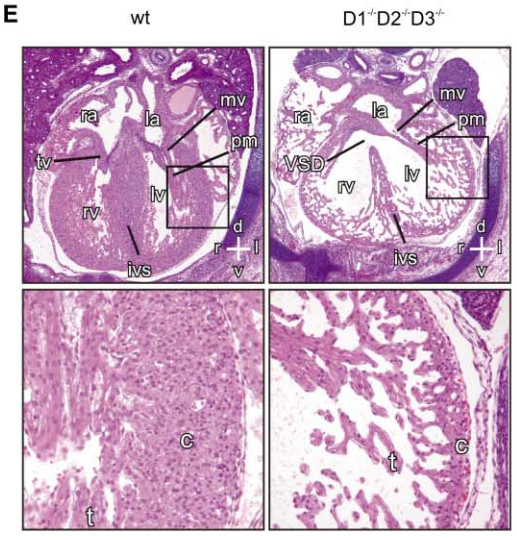

Figure 1. Phenotype of Cyclin D1$^{-/-}$D2$^{-/-}$D3$^{-/-}$ Mice

(A and B) Appearance of cyclin D1$^{-/-}$D2$^{-/-}$D3$^{-/-}$ mice at embryonal day E13.5 (A) and E15.5 (B). Control littermates are shown for comparison.

(C) The ratios of the observed live cyclin D1$^{-/-}$D2$^{-/-}$D3$^{-/-}$ embryos to the total number of embryos analyzed at different stages of embryonic development. The numbers in parentheses refer to dead D1$^{-/-}$D2$^{-/-}$D3$^{-/-}$ embryos.

(D) Bromodeoxyuridine incorporation in E13.5 embryos. Shown are sections through the developing retinas (R), neuroepithelium (N), vertebral cartilages (V), and livers (L).

(E) Cardiac malformations in E15.5 cyclin D1$^{-/-}$D2$^{-/-}$D3$^{-/-}$ embryos.

Upper panels: Histological transverse sections through the heart in the plane of the mitral valve (mv) and papillary muscle (pm). Cyclin D1$^{-/-}$D2$^{-/-}$D3$^{-/-}$ embryos show greatly reduced thickness of the compact zone and a large ventricular septal defect (VSD). Magnification, 25×.

Lower panels: High-power view of wild-type and mutant hearts from the area indicated by the box in the upper panels. The compact (c) and trabecular (t) zones of the myocardial wall are indicated. Magnification, 100×. Axes: d, dorsal; v, ventral; r, right; l, left; ra, right atrium; la, left atrium; rv, right ventricle; lv, left ventricle; ivs, interventricular septum; tv, tricuspid valve.

peared very pale (Figure 1B). No live cyclin D1$^{-/-}$D2$^{-/-}$D3$^{-/-}$ embryos were observed after E16.5 (Figure 1C).

In order to gauge the proliferation of cyclin D-deficient tissues, we stained E13.5 embryonal sections for bromodeoxyuridine (BrdU) incorporation. As shown in the upper three panels of Figure 1D, the proliferation of most tissues in cyclin D1$^{-/-}$D2$^{-/-}$D3$^{-/-}$ embryos was very

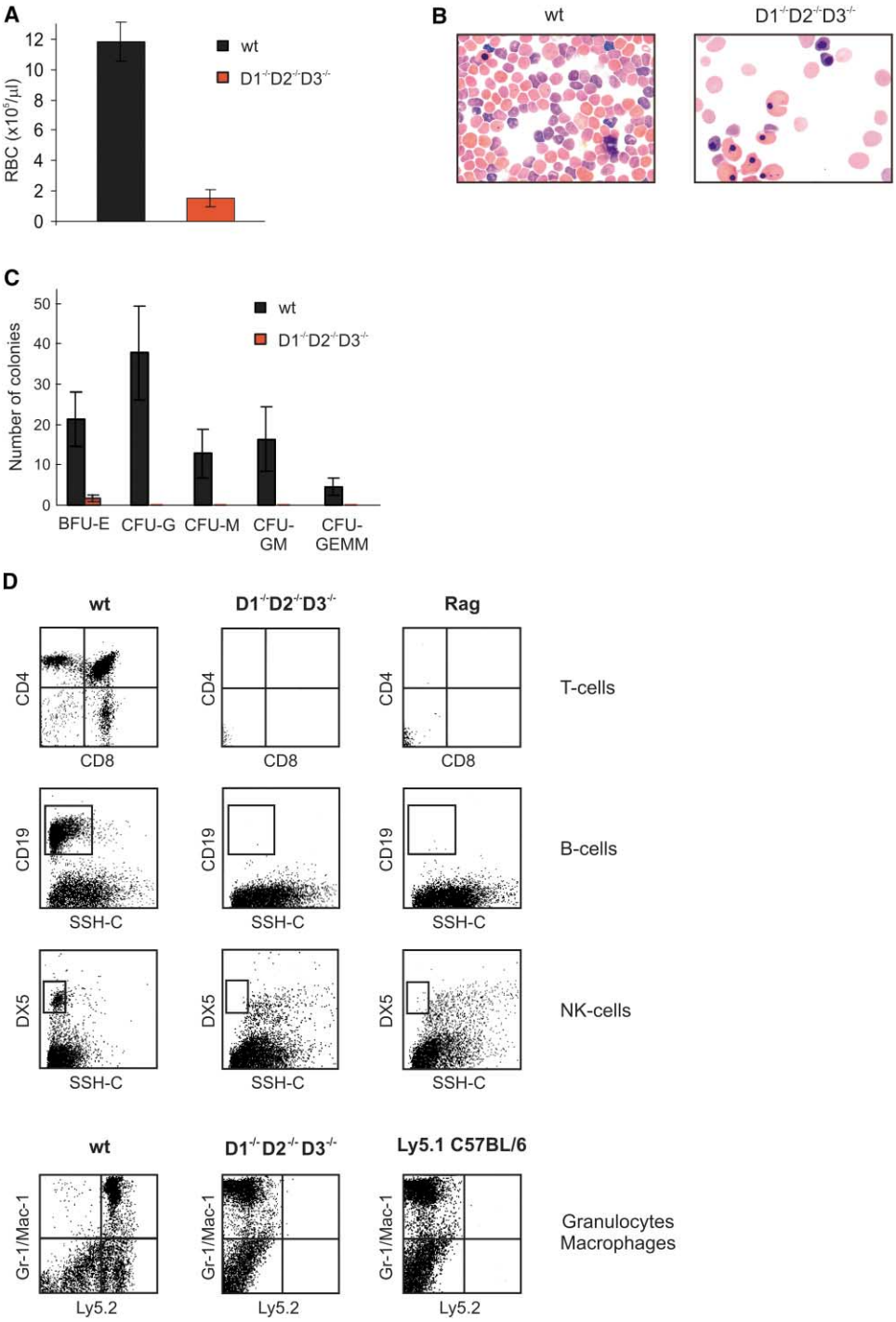

Figure 2. Hematopoietic Abnormalities in Cyclin $D1^{-/-}D2^{-/-}D3^{-/-}$ Embryos

(A) Mean numbers of erythrocytes (RBC) per microliter of peripheral blood in E14.5 wild-type (wt, n = 3) and cyclin $D1^{-/-}D2^{-/-}D3^{-/-}$ (n = 3) mice. Error bars denote SD.

(B) Representative peripheral blood smears of E14.5 wild-type (wt) and cyclin $D1^{-/-}D2^{-/-}D3^{-/-}$ mice stained with Giemsa.

(C) The mean number of myeloid colonies in methylcellulose cultures. 2×10^4 of wild-type (wt, n = 3) or cyclin $D1^{-/-}D2^{-/-}D3^{-/-}$ fetal liver cells (n = 3) were plated in duplicate. Colonies were counted after 12 to 14 days. BFU-E, burst-forming unit erythroid; CFU-G, CFU-M, CFU-GM, and CFU-GEMM, colony-forming unit granulocyte, macrophage, granulocyte-macrophage, granulocyte-erythroid-megakaryocyte-macrophage. Error bars denote SD.

(D) *Upper row*: Flow cytometric analyses of thymocytes isolated from intact $Rag1^{-/-}\gamma c^{-/-}$ mice (Rag), $Rag1^{-/-}\gamma c^{-/-}$ mice that received wild-type fetal liver cells (wt), or $Rag1^{-/-}\gamma c^{-/-}$ mice that received cyclin $D1^{-/-}D2^{-/-}D3^{-/-}$ fetal liver cells.

Second row: Similar analyses of B lymphocytes isolated from bone marrow. SSH-C, side scatter.

Third row: Similar analyses of natural killer cells isolated from spleens.

Fourth row: Analyses of $Gr\text{-}1^+/Mac\text{-}1^+$ cells in the bone marrow of intact Ly5.1 C57BL/6 mice (Ly5.1 C57BL/6), Ly5.1 C57BL/6 mice that received wild-type fetal liver cells (wt), or Ly5.1 C57BL/6 mice that received cyclin $D1^{-/-}D2^{-/-}D3^{-/-}$ fetal liver cells. Cells were stained with antibodies against Ly5.2 and Gr-1/Mac-1. Donor-derived cells are Ly5.2 positive, recipients are Ly5.2 negative.

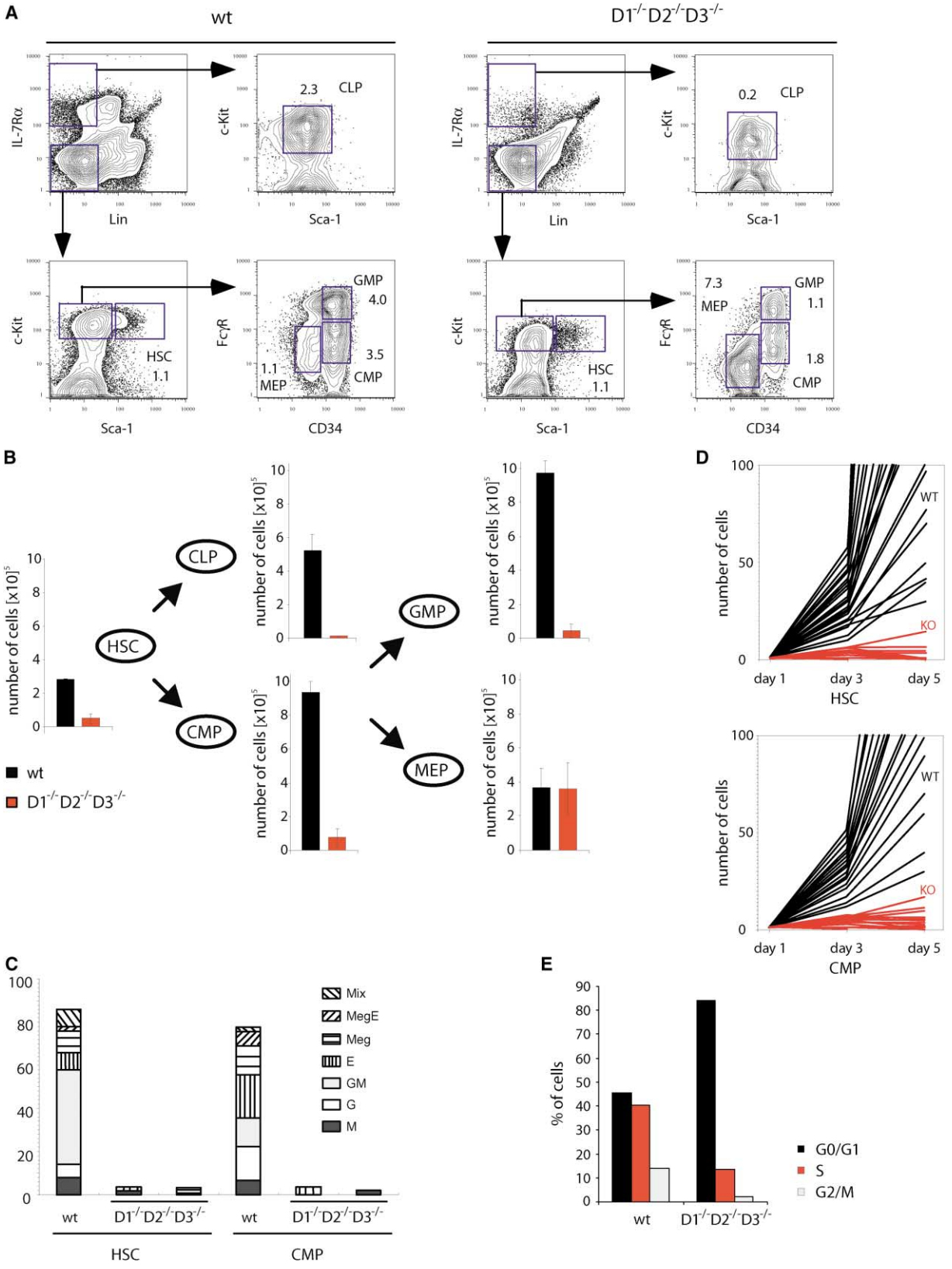

Figure 3. Analyses of Hematopoietic Stem Cells and Lineage-Committed Progenitors

(A) Cells were isolated from fetal livers of E14.5 embryos and were stained for the presence of hematopoietic stem cells (HSC), common lymphoid progenitors (CLP), common myeloid progenitors (CMP), granulocyte-macrophage progenitors (GMP), and megakaryocyte-erythroid progenitors (MEP). The percentages of particular populations among all fetal liver cells are indicated.

comparable to that seen in their wild-type counterparts. These results indicate that normal cell proliferation can occur in the absence of D-cyclins.

Phenotypes of Cyclin D-Deficient Mice

Histopathologic analyses of serially sectioned mutant embryos revealed normal morphogenesis in nearly all major organs and in the extraembryonal tissues, including placentas (data not shown). Hence, the overwhelming majority of compartments can develop normally, at least until this stage, in the absence of all D-cyclins.

An exception to this rule was provided by our observations that mutant embryos displayed severely thinned walls of the heart ventricles, mainly affecting the compact zone (Figure 1E). In addition, cyclin D1$^{-/-}$D2$^{-/-}$D3$^{-/-}$ hearts showed a ventricular septal defect (Figure 1E), an abnormality often seen in mutants with compact zone deficiency (Sucov, 1998). These lesions most likely reflect proliferative failure of myocardial cells. The profound cardiac abnormalities in cyclin D1$^{-/-}$D2$^{-/-}$D3$^{-/-}$ embryos resulted in a severe cardiac output failure, as evidenced by generalized edema (data not shown), and likely contributed to the lethality seen in cyclin D-deficient embryos.

Pale appearance of cyclin D1$^{-/-}$D2$^{-/-}$D3$^{-/-}$ embryos suggested that anemia might also contribute to the demise of mutant conceptuses. Indeed, we found that the number of peripheral blood erythrocytes was reduced almost 8-fold in mutant embryos (Figure 2A). Importantly, some mature, enucleated erythrocytes were encountered in the mutant blood (Figure 2B), revealing that limited definitive erythropoiesis does take place in cyclin D-deficient animals, albeit at a very inefficient rate.

We concluded that a severe anemia, together with a cardiac output failure, leads to lethality of mutant embryos prior to day E17.5 of gestation.

Hematopoietic Abnormalities in Cyclin D1$^{-/-}$D2$^{-/-}$D3$^{-/-}$ Embryos

We next asked whether the hematopoietic abnormalities seen in cyclin D-deficient mice were restricted only to the erythroid lineage or, alternatively, other hematopoietic compartments were also affected. At embryonal day 14.5, fetal livers represent the major site of hematopoiesis, and they contain multipotent hematopoietic stem cells that are able to give rise to all myeloid and lymphoid lineages (Morrison et al., 1995). We first isolated fetal liver cells from wild-type and cyclin D-deficient embryos and determined that the number of these cells was reduced 4.7-fold in mutant animals ($5.5 \pm 3 \times 10^6$, n = 9 in cyclin D1$^{-/-}$D2$^{-/-}$D3$^{-/-}$, versus $25.6 \pm 2.7 \times 10^6$, n = 5 in wild-type). We next plated equal numbers of wild-type or cyclin D1$^{-/-}$D2$^{-/-}$D3$^{-/-}$ fetal liver cells in methylcellulose in the presence of various cytokines, and we tested the ability of hematopoietic progenitors to form colonies. Consistent with a severe anemia seen in cyclin D-deficient mice, we found that the number of erythroid burst-forming units (BFU-E) was reduced 12.7-fold in mutant embryos (Figure 2C). Strikingly, we found that cyclin D-deficient embryos were completely devoid of all other myeloid progenitors, such as CFU-G (colony-forming unit granulocytes), CFU-M (macrophages), CFU-GM (granulocytes/macrophages), and CFU-GEMM (mixed lineage including granulocytes, macrophages, erythrocytes, and megakaryocytes) (Figure 2C). These results suggested a profound multilineage hematopoietic failure in mutant animals.

To probe this phenotype further, we performed bone marrow reconstitution assays. In this procedure, fetal liver cells are injected into tail veins of irradiated recipients, and the ability of hematopoietic stem cells to reconstitute various lymphoid and myeloid lineages is measured (Morrison et al., 1995). A successful long-term reconstitution indicates the presence of functional stem cells in donors' fetal livers. Conversely, absence of the reconstitution suggests a stem cell failure in the donor animals (Park et al., 2003).

In the first set of experiments, we injected equal numbers of wild-type or cyclin D1$^{-/-}$D2$^{-/-}$D3$^{-/-}$ fetal liver cells into irradiated Rag1$^{-/-}\gamma$c$^{-/-}$ mice, and we measured the contribution of the fetal cells to the lymphoid lineages. Importantly, Rag1$^{-/-}\gamma$c$^{-/-}$ mice lack T and B lymphocytes as well as natural killer (NK) cells (Figure 2D), hence all the lymphoid cells in the reconstituted mice are donor derived (Colucci et al., 2000). As expected, injection of Rag1$^{-/-}\gamma$c$^{-/-}$ mice with wild-type fetal liver cells led to the reconstitution of all lymphoid compartments (Figure 2D and data not shown). In contrast, mice reconstituted with cyclin D1$^{-/-}$D2$^{-/-}$D3$^{-/-}$ fetal liver cells presented empty lymphoid gates and lacked any T cells, B cells, and NK cells (Figure 2D and data not shown). Hence, cyclin D-deficient fetal liver cells are unable to contribute to the lymphoid compartment.

We next injected equal numbers of wild-type or cyclin D1$^{-/-}$D2$^{-/-}$D3$^{-/-}$ fetal liver cells into irradiated C57BL6 Ly5.1 wild-type recipients. In this approach, the donor and recipient animals express different haplotypes of the Ly5 antigen on the surface of their hematopoietic cells, thereby allowing unequivocal distinction of donor derived (Ly5.2 positive) from the host (Ly5.1 positive) cells (Spangrude and Scollay, 1990). To assess ability of fetal liver cells to reconstitute various myeloid and lymphoid lineages, we analyzed peripheral blood of the recipients at 5, 10, and 15 weeks after the injections. We sacrificed the recipient animals at the end of a 15-week observation period and analyzed their bone mar-

(B) The bars represent total, absolute numbers of HSC, CLP, CMP, GMP, and MEP, calculated per liver, in wild-type and cyclin D1$^{-/-}$D2$^{-/-}$D3$^{-/-}$ embryos. Error bars, SD.

(C) HSC or CMP were flow-sorted from the E14.5 fetal livers, as shown in (A), plated one-cell-per-well in 60 well plates and cultured in the presence of cytokines. The percentage of cells that expanded to form colonies is shown. Colonies were individually picked and stained with Giemsa. The type of the colonies is shown on the graph.

(D) HSC or CMP were plated at one-cell-per-well, as described in (C), and the number of cells per colony was enumerated.

(E) HSC were flow-sorted from the E14.5 fetal livers, as shown in (A), and their cell cycle status was determined by propidium iodide staining followed by FACS analysis. Shown are percentages of cells in various stages of cell cycle progression.

rows and spleens. As expected, wild-type fetal liver cells robustly reconstituted the lymphoid and myeloid (Mac1$^+$ and Gr1$^+$) compartments of the recipient animals. In contrast, no donor-derived lymphoid or myeloid cells were present in the recipients of cyclin D1$^{-/-}$D2$^{-/-}$D3$^{-/-}$ liver cells (Figure 2D and data not shown). Thus, cyclin D-deficient liver cells were unable to reconstitute the hematopoietic lineages, suggesting an absence or greatly reduced levels of functional hematopoietic stem cells in cyclin D1$^{-/-}$D2$^{-/-}$D3$^{-/-}$ fetal livers.

Analyses of Hematopoietic Stem Cells

During normal hematopoietic development, hematopoietic stem cells (HSC) give rise to common lymphoid progenitors (CLP), which expand and produce pre-B and pre-T cells (Figure 3B) (Kondo et al., 1997). Alternatively, HSC differentiate along the myeloid pathway, giving rise to lineage-committed common myeloid progenitors (CMP), which in turn produce granulocyte-macrophage progenitors (GMP) and megakaryocyte-erythroid progenitors (MEP) (Figure 3B) (Akashi et al., 2000; Traver et al., 2001).

One possible explanation for the inability of cyclin D-deficient fetal liver cells to reconstitute hematopoietic lineages was the paucity of hematopoietic stem cells in cyclin D1$^{-/-}$D2$^{-/-}$D3$^{-/-}$ animals. Alternatively, mutant embryos might contain normal numbers of HSC, but the expansion and differentiation of these cells into various lineages might be crippled in the absence of D-cyclins. To distinguish between these possibilities, we took advantage of the fact that HSC, as well as lineage-committed progenitors, can be prospectively isolated from the fetal livers based on their surface markers (Morrison et al., 1995; Traver et al., 2001). We isolated cells from wild-type and cyclin D1$^{-/-}$D2$^{-/-}$D3$^{-/-}$ E14.5 livers and determined the numbers of HSC and of various progenitors in these samples (Figure 3A). Our analyses revealed that cyclin D1$^{-/-}$D2$^{-/-}$D3$^{-/-}$ livers do contain HSC, but their absolute numbers (calculated per liver) were reduced approximately 5.7-fold in the mutant animals (Figures 3A and 3B). As a result, the numbers of lineage-committed progenitors were profoundly affected in the absence of D-cyclins. Thus, the total number of myeloid progenitors, such as CMP and GMP, was reduced over 12-fold and 20-fold, respectively, while the number of CLP was reduced 46-fold in the mutant animals (Figure 3B). Interestingly, the numbers of MEP remained unchanged in cyclin D-deficient embryos (Figure 3B), suggesting that the severe anemia in mutant mice is contributed by the impaired expansion of these progenitors. Consistent with this notion, we observed reduced proliferation rates in cyclin D1$^{-/-}$D2$^{-/-}$D3$^{-/-}$ fetal livers (Figure 1D), i.e., organs composed at this stage mostly of the erythroid lineage.

We wished to directly test whether cyclin D1$^{-/-}$D2$^{-/-}$D3$^{-/-}$ HSC, while reduced in numbers, are able to expand and to give rise to mature cells. To address this issue, we purified HSC from wild-type and cyclin D1$^{-/-}$D2$^{-/-}$D3$^{-/-}$ livers, plated single cells (one cell per well), and cultured them in vitro in the presence of a cocktail of cytokines (Akashi et al., 2000). As expected, nearly 90% of wild-type HSC cells gave rise to hematopoietic colonies containing cells of multiple lineages. In contrast, only 5% of cyclin D1$^{-/-}$D2$^{-/-}$D3$^{-/-}$ HSC expanded to form small colonies (Figure 3C). Sequential enumeration of the number of cells in individual colonies revealed that wild-type HSC underwent multiple cell divisions and formed colonies containing more then 1000 cells on day 5. In contrast, the very few cyclin D1$^{-/-}$D2$^{-/-}$D3$^{-/-}$ stem cells that succeeded to expand in vitro gave rise to colonies containing less than 10 cells (Figure 3D).

Virtually identical results were obtained when the expansion of single cell cultures of CMP was assayed. Again, over 80% of wild-type CMP gave rise to myeloid colonies, containing up to 1000 cells per colony. In contrast, no more than 5% of cyclin D1$^{-/-}$D2$^{-/-}$D3$^{-/-}$ CMP expanded in vitro, producing colonies containing no more than 15 cells (Figures 3C and 3D).

Lastly, we wished to gauge the in vivo proliferative status of HSC in cyclin D-deficient embryos. We flow-sorted HSC from wild-type and cyclin D1$^{-/-}$D2$^{-/-}$D3$^{-/-}$ livers, and we determined their cell cycle distribution by propidium iodide staining. Consistent with our in vitro observations, we found that the fraction of HSC in the S and G2/M phases of the cell cycle was severely crippled in mutant embryos (Figure 3E). Collectively, these results indicate that cyclin D1$^{-/-}$D2$^{-/-}$D3$^{-/-}$ livers contain reduced numbers of HSC and of lineage-committed hematopoietic progenitors, and the ability of these cells to proliferate is profoundly impaired in the absence of D-cyclins. This, together with relatively normal proliferation rates and grossly normal development of other embryonal tissues (except for the heart), reveals a unique requirement for the D-cyclins in the hematopoietic lineage.

Molecular Analyses of Cyclin D1$^{-/-}$D2$^{-/-}$D3$^{-/-}$ Embryos

We next focused on nonhematopoietic tissues that developed normally in cyclin D1$^{-/-}$D2$^{-/-}$D3$^{-/-}$ embryos. In an attempt to understand the molecular basis of this cyclin D-independent proliferation, we prepared lysates from wild-type and cyclin D-deficient tissues, and we determined the levels of cyclins, CDKs, and cell cycle inhibitors. As expected, cyclin D1$^{-/-}$D2$^{-/-}$D3$^{-/-}$ embryos lacked D-type cyclins (Figure 4A). Importantly, the levels of other cell cycle regulators, as well as the activities of cyclin E- and cyclin A-associated kinase activities were essentially unchanged in mutant embryos (Figure 4A). Hence, at least at this level of resolution, no substantial alterations of the cell cycle machinery took place in cyclin D1$^{-/-}$D2$^{-/-}$D3$^{-/-}$ embryos. We noted that mutant embryos continued to express cyclin-dependent kinases CDK4 and CDK6, which normally associate with the D-type cyclins (Sherr and Roberts, 1999). We speculated that in cyclin D1$^{-/-}$D2$^{-/-}$D3$^{-/-}$ cells, these CDKs might instead interact with other cyclins. Such "partner switching" might explain relatively normal development of cyclin D-deficient embryos.

To address this possibility, we determined the association of CDK4 with various cyclins by immunoprecipitation—Western blotting. As expected, CDK4 associated

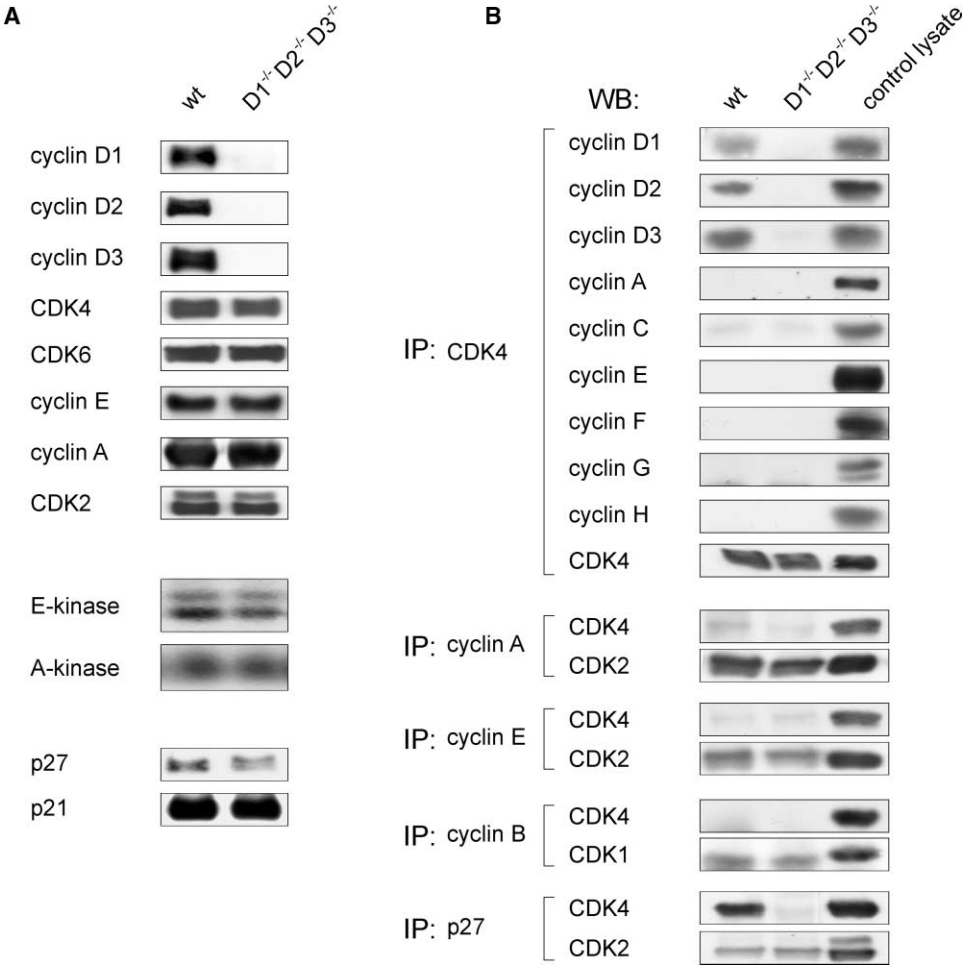

Figure 4. Molecular Analyses of Cyclin D1$^{-/-}$D2$^{-/-}$D3$^{-/-}$ Embryos

(A) Lysates prepared from E13.5 wild-type (wt) or cyclin D1$^{-/-}$D2$^{-/-}$D3$^{-/-}$ embryos were immunoblotted and probed with the indicated antibodies.

(B) Immunoprecipitation (IP)—Western blotting (WB) analyses of E13.5 embryos with the indicated antibodies.

exclusively with cyclins D1, D2, and D3 in the wild-type embryos (Figure 4B). In cyclin D1$^{-/-}$D2$^{-/-}$D3$^{-/-}$ embryos, CDK4 did not partner with the D-type cyclins, which were deleted, but it also did not associate with cyclins A, B, C, E, F, G, and H (Figure 4B). Importantly, control experiments verified the association of these cyclins with their normal catalytic partners in wild-type and in mutant tissues (Figure 4B).

An important function of cyclin D-CDK4/6 complexes is to sequester p27^{Kip1} (and p21^{Cip1}) from cyclin E-CDK2 and cyclin A-CDK2 molecules, thereby triggering kinase activities associated with cyclins E and A (Sherr and Roberts, 1999). We asked whether CDK4 retained the ability to sequester p27^{Kip1} in cyclin D1$^{-/-}$D2$^{-/-}$D3$^{-/-}$ embryos. While we detected abundant association of p27^{Kip1} with CDK4 in wild-type samples, no p27^{Kip1}-CDK4 interaction was detected in cyclin D1$^{-/-}$D2$^{-/-}$D3$^{-/-}$ embryo lysates (Figure 4B). Importantly, control immunoprecipitations revealed normal binding of p27^{Kip1} to CDK2 in mutant samples (Figure 4B). These results suggested to us that the proliferation of cyclin D1$^{-/-}$D2$^{-/-}$D3$^{-/-}$ embryos might occur in a CDK4- (and CDK6-) independent fashion.

Resistance of Cyclin D1$^{-/-}$D2$^{-/-}$D3$^{-/-}$ Cells to p16^{INK4a}

We reasoned that if the proliferation of cyclin D1$^{-/-}$D2$^{-/-}$D3$^{-/-}$ cells occurs in a truly CDK4- and CDK6-independent fashion, these mutant cells would be resistant to p16^{INKa}, an inhibitor of CDK4 and CDK6 (Sherr and Roberts, 1999). To test this possibility, we prepared fibroblasts (MEFs) from day E13.5 cyclin D1$^{-/-}$D2$^{-/-}$D3$^{-/-}$ embryos. Mutant MEFs actively proliferated in culture, although their S phase fraction was decreased, and the G1 fraction was increased as compared with wild-type cells; the proliferation rate of cyclin D1$^{-/-}$D2$^{-/-}$D3$^{-/-}$ cells in vitro was in the range of 60%–80% of that seen in wild-type cells (Figures 5A and 6C, right panel). We next infected wild-type and cyclin D1$^{-/-}$D2$^{-/-}$D3$^{-/-}$ MEFs with retroviruses encoding p16^{INKa}, and we determined the impact of p16^{INK4a} expression on cell proliferation. As expected, expression of

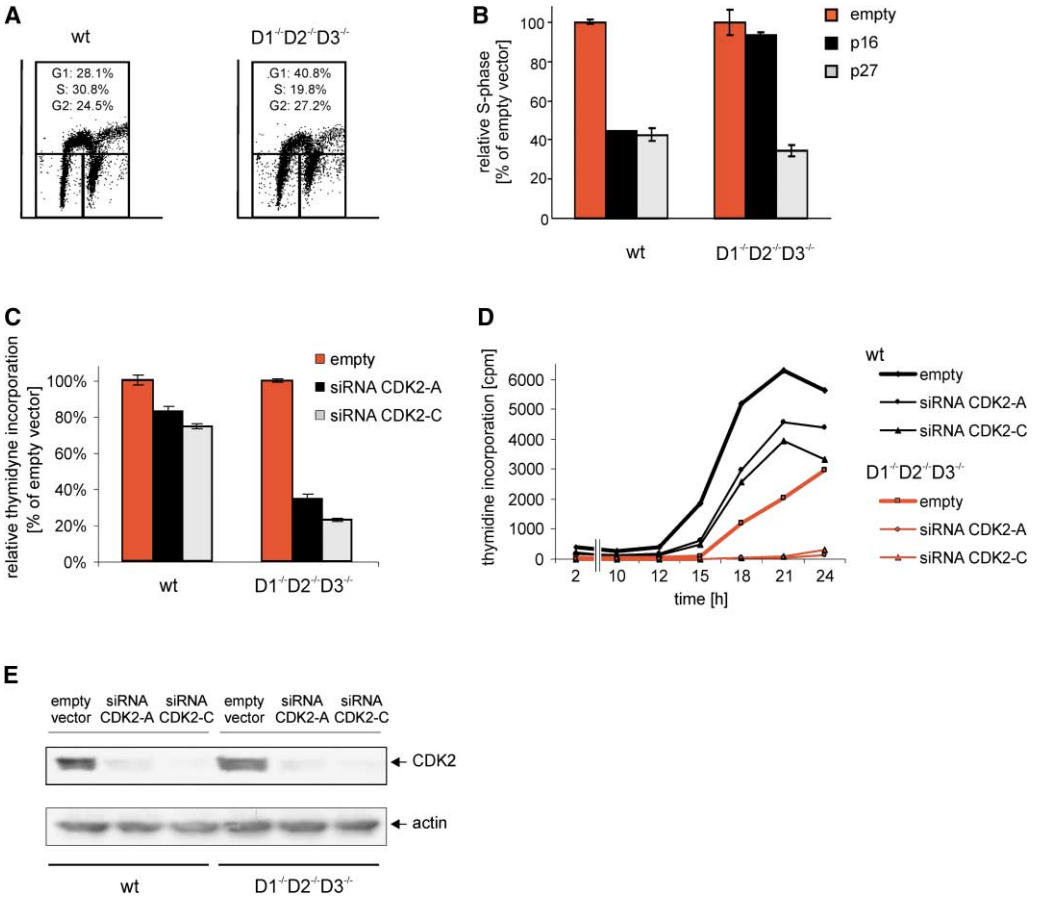

Figure 5. Proliferation of Cyclin D1$^{-/-}$D2$^{-/-}$D3$^{-/-}$ Cells Is Resistant to p16^{INK4a} but Sensitive to CDK2 siRNA

(A) Cell cycle distribution of asynchronously growing mouse embryo fibroblasts (MEFs) cultured in vitro. Cells were pulsed with bromodeoxyuridine (BrdU) for 1 hr and then stained with anti-BrdU antibody and with propidium iodide (PI) followed by FACS analysis. The percentages of cells in particular phases of cell cycle are shown.

(B) MEFs were infected with retroviruses encoding p16^{INK4a} or p27^{Kip1}, or with an empty vector, and the fraction of cells in the S phase was scored by staining cells with PI followed by FACS. Results are shown as relative to S phase fraction of cells infected with an empty vector, which was set as 100%. Error bars denote SD.

(C) MEFs were infected with retroviruses encoding two independent siRNAs against CDK2 (CDK2-A and CDK2-C), or with an empty vector, and the effect on proliferation was gauged by determining [^{3}H]thymidine uptake. Results are shown as relative to proliferation of cells infected with an empty vector, which was set as 100%. Error bars denote SD.

(D) MEFs were infected with retroviruses encoding anti-CDK2 siRNAs, CDK2-A, or CDK2-C, or with the empty vector. Cells were serum starved and then stimulated by serum. Re-entry of cells into the cell cycle was gauged by determining [^{3}H]thymidine uptake.

(E) Western blot analyses of MEFs infected with retroviruses encoding indicated anti-CDK2 siRNA, or with control vector, probed with antibodies against CDK2 or actin (loading control). Note that CDK2-C is more efficient than CDK2-A in bringing down CDK2 levels.

p16^{INK4a} inhibited the proliferation of wild-type cells. In contrast, cyclin D1$^{-/-}$D2$^{-/-}$D3$^{-/-}$ MEFs were resistant to p16^{Ink4a} inhibition (Figure 5B). Importantly, we verified that mutant cells remained susceptible to the inhibition by p27^{Kip1}, which targets cyclin E- and cyclin A-associated kinases (Figure 5B) (Sherr and Roberts, 1999). These results suggest that the proliferation of cyclin D1$^{-/-}$D2$^{-/-}$D3$^{-/-}$ cells occurs in a CDK4- and CDK6-independent fashion.

Proliferation of Cyclin D1$^{-/-}$D2$^{-/-}$D3$^{-/-}$ Cells Depends on CDK2

Two cyclin-CDK classes operate during the G1 phase progression in mammalian cells: cyclin D-CDK4/6 and cyclin E-CDK2 (Sherr and Roberts, 1999). Our demonstration that cyclin D1$^{-/-}$D2$^{-/-}$D3$^{-/-}$ cells proliferated in CDK4- and CDK6-independent fashion caused us to hypothesize that the proliferation of these cells might be driven by CDK2-containing complexes. To address this possibility, we infected wild-type and cyclin D1$^{-/-}$D2$^{-/-}$D3$^{-/-}$ cells with retroviruses encoding two independent siRNAs against CDK2, and we verified the successful knockdown of CDK2 by Western blotting (Figure 5E). We also verified that the levels of other CDKs were unaffected by this procedure (data not shown). We found that the knockdown of CDK2 had only small effect on the proliferation of wild-type cells, consistent with recent reports (Berthet et al., 2003; Ortega et al., 2003). In contrast, the proliferation of cyclin D1$^{-/-}$D2$^{-/-}$D3$^{-/-}$ cells was strongly inhibited by CDK2 knockdown (Figure 5C). Hence, the proliferation of cyclin D1$^{-/-}$D2$^{-/-}$D3$^{-/-}$ cells is critically dependent on CDK2.

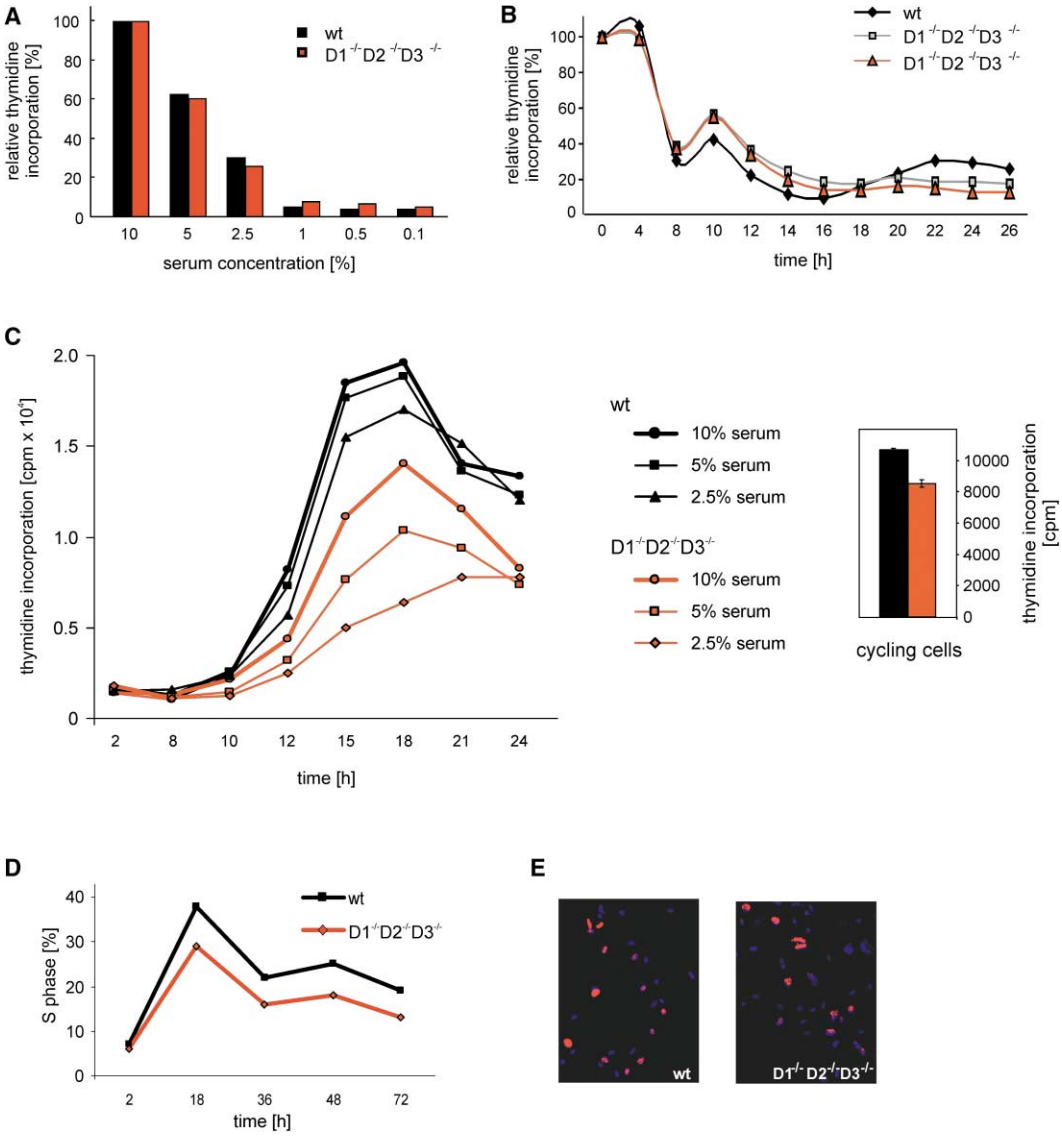

Figure 6. Response of Cyclin D1$^{-/-}$D2$^{-/-}$D3$^{-/-}$ Cells to Extracellular Mitogens

(A) Cells were grown in medium containing decreasing concentrations of serum, and the proliferation was gauged by measuring [^{3}H]thymidine incorporation. Proliferation of cells in 10% serum was set at 100%.

(B) Cells were grown in medium with 10% serum and then were rapidly changed to medium containing no serum. Proliferation was quantitated by measuring [^{3}H]thymidine incorporation. Proliferation of cells in 10% serum (time 0) was set as 100%.

(C) Cells were rendered quiescent by serum deprivation and then re-fed with medium containing indicated concentrations of serum. Entry of cells into the S phase was scored by measuring [^{3}H]thymidine incorporation. Righthand panel shows thymidine incorporation of the very same cells prior to serum starvation (i.e., under conditions of continuous cell growth).

(D) Similar experiment as in (C), using medium with 10% of serum. The percentage of cells in the S phase was determined by staining cells with the propidium iodide followed by FACS.

(E) Cells were rendered quiescent by serum deprivation and then stimulated to re-enter cell cycle by addition of medium with 10% of serum. Cells were fixed after 24 hr and stained with an antibody against phospho-(Ser10) histone H3, a marker of mitotic cells, and co-stained with DAPI.

In an additional approach, we serum starved MEFs that expressed anti-CDK2 siRNA, and then forced them to re-enter cell cycle by serum stimulation. In wild-type cells, knockdown of CDK2 resulted in a slight delay of the S phase entry, consistent with the published results (Berthet et al., 2003; Ortega et al., 2003). In contrast, S phase entry of cyclin D1$^{-/-}$D2$^{-/-}$D3$^{-/-}$ cells was virtually extinguished by both anti-CDK2 siRNAs (Figure 5D). We concluded that in the absence of D-cyclins, the continuous proliferation of cells, as well as their re-entry from the G_0 state is driven by CDK2-containing complexes.

Response of Cyclin D1$^{-/-}$D2$^{-/-}$D3$^{-/-}$ Cells to the Extracellular Environment

D-cyclins are assumed to represent critical cell cycle "sensors" of the extracellular mitogenic environment. Hence, we tested the response of cells lacking D-cyclins to changes in the external mitogenic stimulation. First,

we cultured cells in medium containing decreasing concentrations of serum and gauged the rate of proliferation by measuring [^{3}H]thymidine uptake. We found that cyclin D1$^{-/-}$D2$^{-/-}$D3$^{-/-}$ MEFs responded to reduced mitogenic stimulation in a pattern that was essentially identical to that seen in wild-type cells (Figure 6A).

We next rapidly switched cells grown in serum-rich (10%) medium to serum-free medium, and we followed the response. Again, both wild-type and cyclin D1$^{-/-}$D2$^{-/-}$D3$^{-/-}$ cells responded very similarly and exited the cell cycle with virtually identical kinetics (Figure 6B).

Lastly, we analyzed the ability of cyclin D1$^{-/-}$D2$^{-/-}$D3$^{-/-}$ cells to re-enter cell cycle from the quiescent state. We arrested cells in the G_0 phase by serum deprivation and triggered cell cycle re-entry by the addition of media containing different concentrations of serum. Stimulation of mutant cells with medium containing 10% of serum led to a robust S phase entry, with a similar kinetics as that seen in wild-type cells (Figures 6C and 6D). We verified that cyclin D1$^{-/-}$D2$^{-/-}$D3$^{-/-}$ cells traversed the S and G2 phases, entered mitosis (as documented by phospho-histone H3 staining, Figure 6E), and eventually divided, resulting in an increase in cell numbers (data not shown). Hence, mutant MEFs can exit quiescence, re-enter the S, G2, and M phases, and complete a productive cell division in the absence of any cyclin D activity.

In contrast, stimulation of cells with lower mitogen concentrations (5% and 2.5% of serum) gave a very different outcome. Whereas wild-type cells re-entered the cell cycle with efficiencies close to that observed with 10% of serum, the cell cycle re-entry was clearly reduced in cyclin D1$^{-/-}$D2$^{-/-}$D3$^{-/-}$ cells (Figure 6C). Hence, cyclin D-deficient cells show increased mitogenic requirement for cell cycle re-entry, as compared with wild-type cells.

Activation of Cyclins E and A in the Absence of D-Cyclins

Induction of D-cyclins in response to mitogenic stimulation is believed to drive cell cycle progression by titration of p27^{Kip1} away from cyclin E-CDK and cyclin A-CDK complexes, thereby triggering kinase activity associated with these holoenzymes (Sherr and Roberts, 1999). Nearly normal cell cycle re-entry in cyclin D1$^{-/-}$D2$^{-/-}$D3$^{-/-}$ cells stimulated with serum-rich medium prompted us to analyze how these molecular events take place in the absence of D-cyclins. We serum starved cells, stimulated to re-enter the cell cycle by addition of serum-rich (10%) medium, and we collected cells at various time points during the G1 phase progression. We found that in cyclin D1$^{-/-}$D2$^{-/-}$D3$^{-/-}$ cells traversing the G1 phase, the levels of p27^{Kip1} were reduced, as compared with the levels seen in wild-type cells (Figure 7A). Reduction of p27^{Kip1} levels resulted in modest derepression of cyclin E-associated kinase activity at the early stages of cell cycle progression (Figure 7A). However, the sharp, sudden induction of cyclin E- and cyclin A-associated kinase activities proceeded normally in the absence of D-cyclins (Figure 7A). Hence, an additional cyclin D-independent mechanism, which links extracellular mitogenic stimulation with the sudden activation of cyclin E-CDK2 and cyclin A-CDK2 at the G1/S boundary, operates in mammalian cells.

Phosphorylation of the Retinoblastoma Protein

In addition to controlling the activity of cyclin E and cyclin A, cyclin D-CDK complexes were shown to phosphorylate the retinoblastoma protein, pRB (Sherr and Roberts, 1999). For this reason, we gauged pRB phosphorylation during cell cycle progression of cyclin D1$^{-/-}$D2$^{-/-}$D3$^{-/-}$ cells by Western blotting. As expected, the fully phosphorylated pRB species were clearly detectable in wild-type cells at 15 hr poststimulation (Figure 7B). In contrast, the full phosphorylation of pRB was greatly diminished in cyclin D1$^{-/-}$D2$^{-/-}$D3$^{-/-}$ cells (Figure 7B).

We next applied phosphospecific anti-pRB antibodies that allow detecting pRB species that are phosphorylated at particular amino acid residues. We decided to focus on Ser249/Thr252, Ser807/Ser811, and Thr826 since these pRB sites were shown to be phosphorylated exclusively by cyclin D-associated kinases (Zarkowska and Mittnacht, 1997). While all those cyclin D-specific sites were clearly phosphorylated in wild-type cells at the G1/S boundary, their phosphorylation in cyclin D1$^{-/-}$D2$^{-/-}$D3$^{-/-}$ cells was very decreased (Figure 7C).

According to our understanding of the cell cycle progression, the initial phosphorylation of the pRB by cyclin D-CDK complexes is required to allow full phosphorylation of the retinoblastoma protein by the cyclin E- and cyclin A-associated kinases (Harbour et al., 1999; Lundberg and Weinberg, 1998). The absence of significant cyclin D-dependent phosphorylation of pRB molecules in cyclin D1$^{-/-}$D2$^{-/-}$D3$^{-/-}$ cells allowed us to test this model by probing Western blots with two independent antibodies that recognize cyclin E- and A-specific pRB residue, Thr821. Our analyses revealed that this site was phosphorylated in cyclin D1$^{-/-}$D2$^{-/-}$D3$^{-/-}$ cells (Figure 7C and data not shown). Hence, phosphorylation of pRB on cyclin D-specific sites is not required for further phosphorylation, likely by cyclins E and A.

In addition to the retinoblastoma protein, the pRB-related "pocket" proteins p107 and p130 also represent targets for cyclin D-CDK4/6 kinases (Sherr and Roberts, 1999). For this reason, we analyzed the phosphorylation of p107 during cell cycle re-entry of cyclin D1$^{-/-}$D2$^{-/-}$D3$^{-/-}$ cells. As was the case with the retinoblastoma protein, we found that the overall phosphorylation of p107 was clearly diminished in cells lacking D-type cyclins (Figure 7D).

The phosphorylation of the pRB and pRB-related "pocket" proteins leads to the release or derepression of the E2F transcription factors, which in turn control transcription of key target genes required for the S phase entry (Dyson, 1998). Our observations that quiescent cyclin D1$^{-/-}$D2$^{-/-}$D3$^{-/-}$ cells can re-enter the S phase, undergo mitosis, and complete the entire cell division cycle (Figures 6C, 6D, and 6E and data not shown) suggested to us that cyclin E- and cyclin A-driven phosphorylation is sufficient to functionally inactivate the "pocket" proteins and to release the E2Fs. To test this possibility, we measured the induction of known E2F target genes (*cdc2*, *cyclin E*, *thymidylate synthase*, *p107*) during cell cycle re-entry by Northern blotting. We found that transcripts of these E2F targets were induced in cyclin D1$^{-/-}$D2$^{-/-}$D3$^{-/-}$ cells (Figure 7E and data not shown); the maximal degree of induction was lower than that seen in wild-type cells, consistent with the smaller fraction of cells re-entering the S phase in mutant sam-

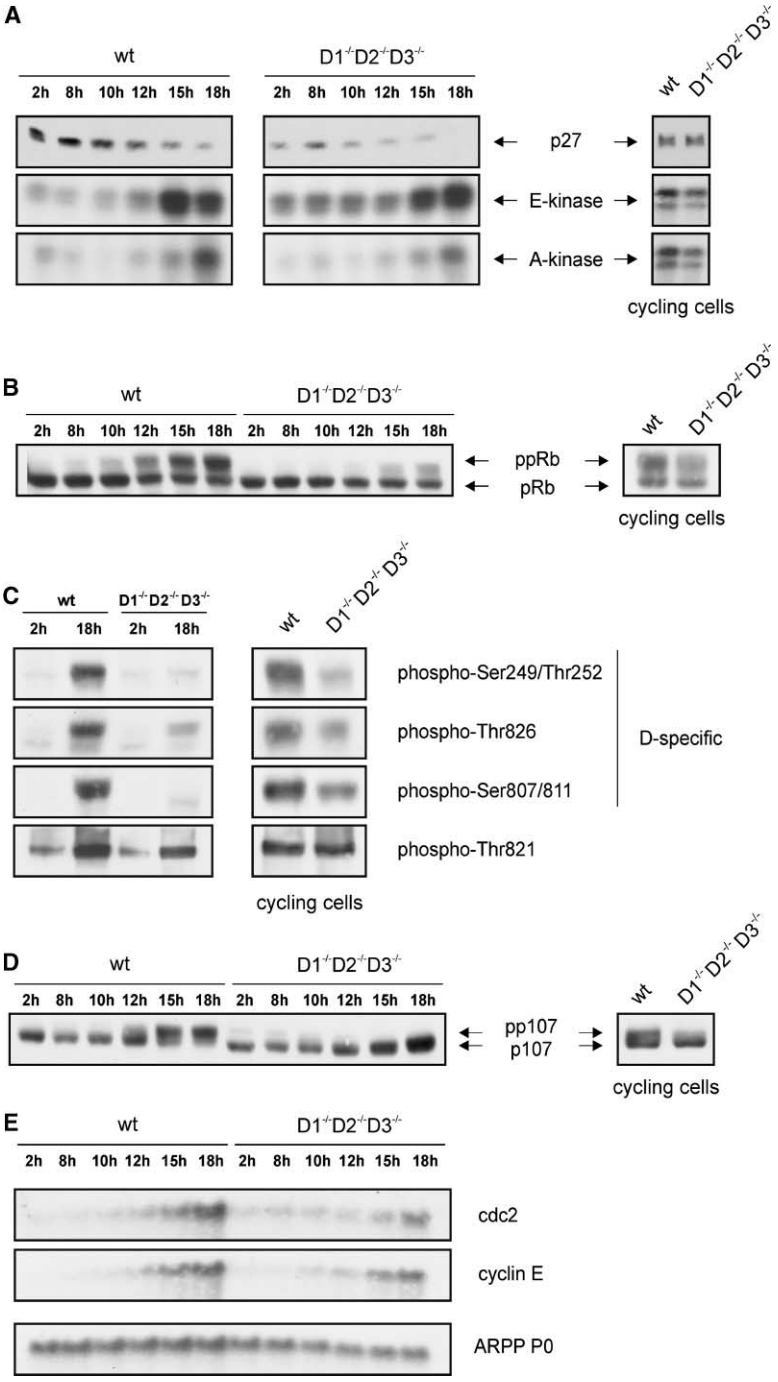

Figure 7. Molecular Analyses of G1 Phase Progression in Cyclin D1$^{-/-}$D2$^{-/-}$D3$^{-/-}$ Cells

(A) *Upper panel:* Cells were serum starved and then stimulated to re-enter cell cycle by addition of medium with 10% serum. Lysates were prepared and immunoblotted with anti-p27^{Kip1} antibody.

Middle and lower panels: Lysates were subjected to immunoprecipitation with antibodies against cyclin E or cyclin A, and kinase activity towards histone H1 was determined. Numbers above the lanes indicate hours after serum stimulation.

(B) Similar experiment as in (A). The immunoblots were probed with an anti-pRB antibody.

(C) Lysates prepared from cells collected at 2 or 18 hr after serum stimulation were used for immunoblotting with anti-phosphospecific antibodies that recognize pRB phosphorylated at particular amino acid residues.

(D) Cells were serum starved and restimulated, as described in (A). Western blots were probed with an anti-p107 antibody.

In (A)–(D), Righthand panels show similar analyses of continuously growing cells.

(E) RNA was prepared from cells at indicated time points after serum stimulation. Northern blots were probed with cDNA probes against indicated E2F targets or with ARPP P0 (loading control).

ples. We concluded that cyclin E- and cyclin A-driven phosphorylation of the "pocket" proteins affords activation of the E2F targets. Together with our demonstration that the proliferation and cell cycle re-entry of cyclin D1$^{-/-}$D2$^{-/-}$D3$^{-/-}$ cells is critically dependent on CDK2, we propose that cyclin E-CDK2 and cyclin A-CDK2 complexes functionally inactivate "pocket" proteins in cyclin D1$^{-/-}$D2$^{-/-}$D3$^{-/-}$ cells.

We noted that in continuously proliferating cyclin D1$^{-/-}$D2$^{-/-}$D3$^{-/-}$ MEFs, the phosphorylation of pRB and p107 was not as strongly affected as in cells re-entering the cell cycle (Figures 7B, 7C, and 7D, right panels). We concluded that in continuously growing cells, kinases other than those associated with D-cyclins (possibly cyclin E-CDK2 and/or cyclin A-CDK2) can bring about some phosphorylation of cyclin D-specific sites on pRB and possibly on p107. It is important to note, however, that the levels of cyclin E- and cyclin A-associated kinase activities are not elevated in continuously proliferating cyclin D1$^{-/-}$D2$^{-/-}$D3$^{-/-}$ MEFs (Figure 7A, right panel).

Reduced Susceptibility of Cyclin D1$^{-/-}$D2$^{-/-}$D3$^{-/-}$ Cells to the Oncogenic Transformation

D-type cyclins were postulated to represent the ultimate recipients of several oncogenic pathways, including the

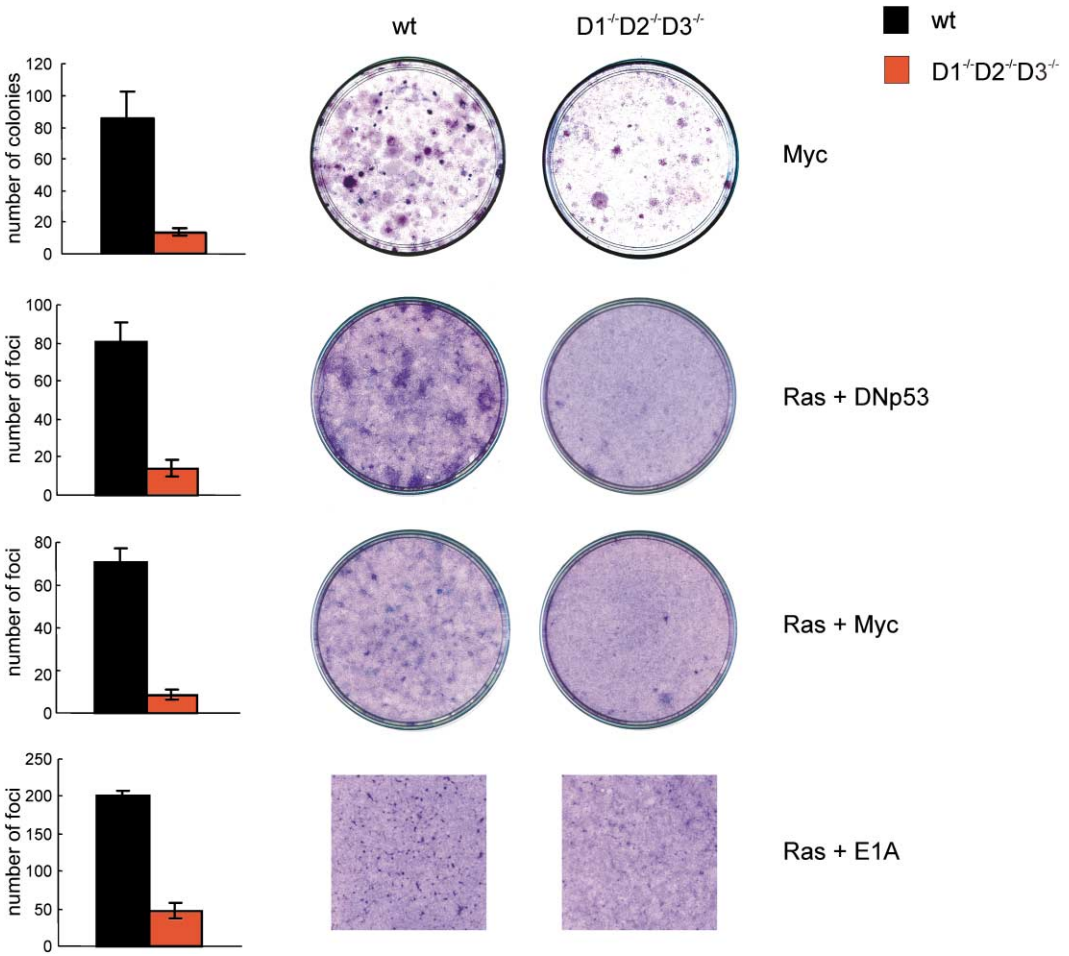

Figure 8. Reduced Sensitivity of Cyclin D1$^{-/-}$D2$^{-/-}$D3$^{-/-}$ Cells to the Oncogenic Transformation

Appearance of crystal violet-stained plates and the mean number of foci or colonies seen in wild-type or cyclin D1$^{-/-}$D2$^{-/-}$D3$^{-/-}$ MEFs infected with retroviruses encoding indicated oncogenes. Error bars denote SD. In case of v-Ha-Ras plus E1A infection, low magnification of the crystal violet-stained monolayers is shown.

ones triggered by the Ras and Myc oncogenes (Bouchard et al., 1999; Perez-Roger et al., 1999; Serrano et al., 1995). This prompted us to test the susceptibility of cells lacking the D-cyclins to various oncogenic insults. To this end, we infected monolayers of cyclin D1$^{-/-}$D2$^{-/-}$D3$^{-/-}$ MEFs with retroviruses encoding Ras plus Myc, Ras plus dominant-negative p53, or Ras plus E1A, and the formation of transformed foci was scored in each experiment. In addition, we infected cells with retroviruses encoding only Myc, and the ability of this oncogene to cause immortalization was analyzed by enumeration of the emerging colonies. We found that cyclin D1$^{-/-}$D2$^{-/-}$D3$^{-/-}$ cells displayed greatly reduced susceptibility to all these oncogenic insults (Figure 8). Hence, the presence of D-cyclins is required to allow full oncogenic transformation, at least by the oncogene combinations analyzed.

Discussion

The three mammalian D-type cyclins show significant amino acid similarity, and they are expressed in an overlapping fashion in all proliferating cell types. After the discovery of the D-type cyclins (Matsushime et al., 1991; Motokura et al., 1991; Xiong et al., 1991), it was initially assumed that each of them is independently required to allow cell proliferation.

In the past, we and others (Fantl et al., 1995) started to address the functions of the D-cyclins by creating mice lacking cyclins D1, D2, or D3. We found that all these strains were viable and displayed narrow, tissue-specific phenotypes. Thus, cyclin D1-deficient mice presented developmental neurological abnormalities and displayed hypoplastic retinas and hypoplastic mammary glands (Fantl et al., 1995; Sicinski et al., 1995). Cyclin D2-deficient females were sterile, owing to ovarian granulosa cell defect, while cyclin D2$^{-/-}$ males displayed hypoplastic testes (Sicinski et al., 1996). In addition, cyclin D2-deficient animals showed cerebellar abnormalities (Huard et al., 1999), impaired proliferation of B lymphocytes (Lam et al., 2000; Solvason et al., 2000), and hypoplasia of pancreatic β cells (J. Kushner, personal communication). Lastly, cyclin D3-deficient mice displayed defects in the development of T lymphocytes (Sicinska et al., 2003). Surprisingly, analyses of

mice lacking combinations of the two D-type cyclins failed to uncover any new phenotypes; instead these "single cyclin" mice displayed combinations of phenotypes associated with the deficiency of individual D-cyclins (Ciemerych et al., 2002). We interpreted these observations as an indication that at least one D-type cyclin is sufficient to allow normal development, and that the narrow, tissue-specific phenotypes of mice lacking individual D-type cyclins reflect the highly overlapping pattern of expression of the three D-type cyclins.

We were puzzled, however, by the unexplained observations that mice lacking catalytic effectors of the D-cyclins, CDK4 and CDK6, display narrow tissue-specific abnormalities that affect the very similar compartments to those crippled in cyclin D-deficient animals. Thus, CDK4-deficient mice show developmental neurological abnormalities that are similar to those observed in cyclin D1 null animals and present ovarian and testicular abnormalities and pancreatic β cell hypoplasia like cyclin $D2^{-/-}$ mice (Rane et al., 1999; Tsutsui et al., 1999). CDK6-deficient mice, in turn, present erythroid and lymphoid defects (Malumbres et al., 2004 [this issue of *Cell*]), resembling those observed in cyclin $D3^{-/-}$ animals. Moreover, mice lacking Bmi-1, a repressor of cyclin D-CDK4/6 inhibitor, $p16^{INK4a}$, display hypoplastic cerebella, impaired development of the T lymphocytes, and other hematopoietic abnormalities, again resembling the phenotypes seen in cyclin D1-, D2-, or D3-deficient mice (Jacobs et al., 1999; Park et al., 2003).

In the work described here, we provide evidence that the development of the majority of mouse tissues can occur in a cyclin D-independent fashion. We found that the function of D-cyclins is critically required for development only in few selected compartments. Importantly, the very same compartments require CDK4 and CDK6, as evidenced by very similar phenotypes of cyclin $D1^{-/-}D2^{-/-}D3^{-/-}$ mice (this study) and $CDK4^{-/-}$ $CDK6^{-/-}$ animals (Malumbres et al., 2004). Collectively, these observations provide genetic evidence that the major function of the D-cyclins in development is to activate CDK4 and CDK6, and they unexpectedly reveal that the majority of mammalian cell types can develop and proliferate in the absence of cyclin D-CDK4/6 activity. One of the major challenges in the field will be to identify the differences in the cell cycle machinery of "cyclin D-dependent" versus "cyclin D-independent" cell types.

The notion that normal proliferation can occur in the absence of cyclin D-CDK4 activity was first proposed by the findings of Cheng et al. (1999), who reported that fibroblasts lacking $p27^{Kip1}$ and $p21^{Cip1}$ can proliferate normally in the absence of any detectable cyclin D-CDK complexes. These findings raised a possibility of cyclin D-independent proliferation in mammalian cells.

In *Caenorhabditis elegans*, the RNAi-mediated inactivation of *cyd-1* or *cdk-4* genes, which encode homologs of mammalian D-cyclins and CDK4/6, respectively, does not interfere with normal embryonal development and only affects proliferation of postembryonic blast cells (Park and Krause, 1999). Likewise, deletion of the *Drosophila melanogaster cdk4* gene, a homolog of mammalian CDK4 and CDK6, affects cell growth rather than cell proliferation and results in viable, smaller flies (Meyer et al., 2000). Hence, the cyclin D-independent mode of proliferation also takes place in nonmammalian cells.

The current notion that mammalian cells critically require D-cyclins for proliferation is largely based on the observations that ectopic overexpression of the INK family of inhibitors ($p16^{INK4a}$, $p15^{INK4b}$, $p18^{INK4c}$, and $p19^{INK4d}$) inhibits proliferation of in vitro cultured cells. However, the major effect of INK inhibitors may be mediated by the liberation of cyclin D-CDK4/6 bound $p27^{Kip1}$ and $p21^{Cip1}$ inhibitors. This mechanism of $p16^{INK4a}$-mediated cell cycle arrest does not take place in cyclin $D1^{-/-}D2^{-/-}D3^{-/-}$ cells, as they do not have cyclin D-CDK4/6 complexes.

We note that in the majority of cell types, $p16^{INK4a}$ inhibited but did not completely block cell cycle progression. In contrast, expression of $p16^{INKa}$ in in vitro cultured hematopoietic stem cells was shown to completely shut off their proliferation (Park et al., 2003). Moreover, mice lacking Bmi-1, a repressor of $p16^{INK4a}$, show elevated levels of $p16^{INK4a}$ and display a profound impairment of hematopoietic stem cell self-renewal (Park et al., 2003). Hence, the proliferation of hematopoietic stem cells, and of few other "D-dependent" compartments, critically requires D-type cyclins. We note here that these Bmi-$1^{-/-}$ mice also display proliferative deficiencies within the neural stem cell compartment (Molofsky et al., 2003). It will be very interesting to determine whether these neural stem cells, and possibly other stem cell types, are also affected in cyclin D null animals.

In contrast to hematopoietic stem cells, the proliferation of fibroblasts proceeded relatively normally in the absence of D-cyclins. Our demonstration that the proliferation of these cells critically depends on CDK2 suggests that cyclin D-CDK4/6 and cyclin E-CDK2 complexes may perform overlapping functions in "cyclin D-independent" cell types. The exact molecular functions of these complexes do not need to be identical. For instance, the retinoblastoma protein contains 16 consensus CDK phosphorylation sites and the majority of them can be phosphorylated by cyclin D-, E-, and A-associated kinases (Zarkowska and Mittnacht, 1997). A small subset of pRB sites can be phosphorylated only by cyclin D-CDK complexes (Zarkowska and Mittnacht, 1997), and these sites remain hypophosphorylated in cyclin $D1^{-/-}D2^{-/-}D3^{-/-}$ cells. However, cyclin E- and A-driven phosphorylation of pRB appears to suffice for the functional inactivation of pRB and allows normal cell cycle progression.

While the activity of cyclin E and A may suffice to allow cell proliferation, an important question is how these cyclins are activated in response to the environmental cues in the absence of the D-type cyclins. Our results clearly indicate the presence of an alternative, cyclin D-independent mechanism that couples the activation of cyclins E and A to the extracellular environment (see Figure 7A). While the molecular basis of this mechanism is currently unknown, cyclin $D1^{-/-}D2^{-/-}D3^{-/-}$ cells offer us a tool to address this issue.

Consistent with the growth-promoting functions for D-cyclins, amplification of the cyclin D genes and overexpression of cyclin D proteins was reported in several human cancers. The most frequent of these is the involvement of cyclin D1 overexpression in the majority of human breast cancers (Weinstat-Saslow et al., 1995). Our demonstration that D-cyclins are dispensable for

proliferation of a great number of cell types, but not for oncogenic transformation by Ras and Myc, may offer a window of opportunity for targeting D cyclins in human malignancies.

Experimental Procedures

Histopathologic Analyses

Organs or embryos were fixed in Bouin's fixative (Sigma) and processed for histology. Bromodeoxyuridine staining was performed as described (Ciemerych et al., 2002). Peripheral blood was obtained from carotid arteries of viable E14.5 embryos. Blood smears were prepared using the wedge technique, followed by air drying and Wright-Giemsa staining.

Methylcellulose Cultures

Livers were collected from E14.5 embryos and single cell suspensions were prepared. Cells were plated in methylcellulose (Stem Cell Technologies #M3434), 2×10^4 cells per dish, plus 50 ng/ml stem cell factor, 10 ng/ml interleukin (IL)-3, 10 ng/ml IL-6, and 3 U/ml erythropoietin. For each sample, two duplicate dishes were analyzed.

In Vivo Reconstitution Assays

$Rag1^{-/-}\gamma c^{-/-}$ mice (Colucci et al., 2000), purchased from Taconics, were irradiated (450 cGy) using ^{137}Cs source. Fetal liver cells were isolated from E14.5 embryos, and 10^6 fetal liver cells were injected into tail veins of $Rag1^{-/-}\gamma c^{-/-}$ recipients (n = 3 for wild-type and for cyclin $D1^{-/-}D2^{-/-}D3^{-/-}$). Animals were sacrificed after 5 weeks. Peripheral blood cells, thymocytes, splenocytes, and bone marrow were stained with antibodies against CD4, CD8, CD19, and DX5. For competitive reconstitution, 10^6 E14.5 fetal liver cells from wild-type (n = 4) or cyclin $D1^{-/-}D2^{-/-}D3^{-/-}$ embryos (n = 4), all $Ly5.2^+$, were mixed with 0.3×10^6 $Ly5.1^+$ bone marrow cells and injected into tail veins of ^{137}Cs-irradiated (950 cGy, split dose) $Ly5.1^+$ C57BL/6 mice. Peripheral blood was collected after 5, 10, and 15 weeks, and bone marrow and splenocytes were collected after 15 weeks. Cells were stained with antibodies against B220, Gr1, and Mac1, along with anti-Ly5.2 antibody, and analyzed by FACS (Spangrude and Scollay, 1990).

Stem Cell and Progenitor Analyses

Myeloid progenitors were sorted as IL-$7R\alpha^-$Lin$^-$Sca-1^-c-Kit^+CD34^+ $Fc\gamma RII/III^{lo}$ (CMP), IL-$7R\alpha^-$Lin$^-$Sca-1^-c-$Kit^+CD34^+Fc\gamma RII/III^{hi}$ (GMP), and as IL-$7R\alpha^-$Lin$^-$Sca-1^-c-$Kit^+CD34^-Fc\gamma RII/III^{lo}$ (MEP) (Akashi et al., 2000). HSC and CLP were sorted as IL-$7R\alpha^-$Lin$^-$Sca-1^{hi}c-Kit^{hi} and IL-$7R\alpha^+$Lin$^-$Sca-1^{lo}c-Kit^{lo} populations, respectively (Kondo et al., 1997) (Figure 3A).

To test myelo-erythroid potential, single cells were sorted into Terasaki plates with IMDM supplemented with 20% FBS, mSlf (20 ng/ml), mIL-3 (10 ng/ml), mIL-11 (10 ng/ml), mGM-CSF (10 ng/ml), mTpo (10 ng/ml), hEpo (1 U/ml). Colonies were enumerated under an inverted microscope consecutively from day 1 to day 5. Types of colonies were determined by Giemsa staining of cells that were picked from individual colonies.

For cell cycle analyses, HSC were sorted as described above, fixed in 70% ethanol, stained with propidium iodide, and the DNA content was analyzed by flow cytometry.

Cell Proliferation Analyses and Oncogene Transformation Assays

These were performed as described (Ciemerych et al., 2002). For $p16^{INK4a}$ and $p27^{Kip1}$ overexpression, cells were infected with pBabe-Puro-$p16^{Ink4a}$ or pBabe-Puro-$p27^{Kip1}$, selected in puromycin for 3 days, and plated at 5×10^4 cells per well in 24 well plate. Proliferation was scored by measuring [^{3}H]thymidine uptake or by staining cells with propidium iodide. For phospho-histone H3 staining, polyclonal anti phospho-(ser 10) histone H3 antibody (Upstate Biotechnology) and FITC-conjugated secondary antibodies (Jackson Immunoresearch Laboratory) were used. Anti-CDK2 siRNAs were designed against the 5′CAUCAAGAGCUAUCUGUUCCA3′ (CDK2-A) or 5′AAG AUGGACGGAGCUUGUUAU3′ (CDK2-C) sequences of the mouse CDK2 transcript. Oligonucleotides were cloned into pMKO.1 retroviral vector. Cells were infected, selected in puromycin for 3 days, and plated for the experiments. Proliferation was scored by measuring [^{3}H]thymidine uptake or by staining cells with propidium iodide.

Western and Northern Blotting

Western blots, immunoprecipitations (IP), or kinase assays were done as described (Ciemerych et al., 2002) using antibodies against cyclins D2, D3, E, F, H, CDK2, CDK4, CDK6, p21, p27, all from Santa Cruz, cyclin A (Sigma), cyclins B, C, D1, CDK1 (NeoMarkers), cyclin G1 (from Dr. P. Hinds), pRB (BD Biosciences), pRB pSer249/Thr252, pRB pThr826 (EMD Biosciences), pRB pSer807/Ser811 (Cell Signaling), pRB pThr821 (Abcam). For IP-kinase assays, we used antibodies against cyclins E or A (Santa Cruz). For Northern blotting, 20 μg of total RNA was resolved on MOPS gels as described (Sicinska et al., 2003) and probed with ^{32}P-labeled cDNA probes.

Acknowledgments

The authors thank R. Kaminski, L. Litowchick, J. DeCaprio, S. Mittnacht, M. Cohn, L. Zhang, L. Callahan, J. Schneider, S. Neubauer, K. Clarke, and the members of the Sicinski lab for help; P. Hinds for anti-cyclin G1 antibody; N. Dyson for the probes for E2F targets; A. Gudkov, S. Lowe, and M. Eilers for the DNp53, Ras, and Myc retroviral constructs; and M. Malumbres and M. Barbacid for communicating unpublished data. M.A.C. was supported by the Yamagiwa-Yoshida Memorial UICC International Cancer Study Grant. V.I.R. was supported by a grant from the Leukemia and Lymphoma Society. This work was supported by grants from the NIH (CA85296 and CA108420) to P.S.

Received: April 2, 2004
Revised: June 20, 2004
Accepted: June 28, 2004
Published: August 19, 2004

References

Akashi, K., Traver, D., Miyamoto, T., and Weissman, I. (2000). A clonogenic common myeloid progenitor that gives rise to all myeloid lineages. Nature *404*, 193–197.

Berthet, C., Aleem, E., Coppola, V., Tessarollo, L., and Kaldis, P. (2003). Cdk2 knockout mice are viable. Curr. Biol. *13*, 1775–1785.

Bouchard, C., Thieke, K., Maier, A., Saffrich, R., Hanley-Hyde, J., Ansorge, W., Reed, S., Sicinski, P., Bartek, J., and Eilers, M. (1999). Direct induction of cyclin D2 by Myc contributes to cell cycle progression and sequestration of p27. EMBO J. *18*, 5321–5333.

Cheng, M., Olivier, P., Diehl, J., Fero, M., Roussel, M., Roberts, J., and Sherr, C. (1999). The p21Cip1 and p27Kip1 CDK 'inhibitors' are essential activators of cyclin D-dependent kinases in murine fibroblasts. EMBO J. *18*, 1571–1583.

Ciemerych, M., Kenney, A., Sicinska, E., Kalaszczynska, I., Bronson, R., Rowitch, D., Gardner, H., and Sicinski, P. (2002). Development of mice expressing a single D-type cyclin. Genes Dev. *16*, 3277–3289.

Colucci, F., Guy-Grand, D., Wilson, A., Turner, M., Schweighoffer, E., Tybulewicz, V., and Di Santo, J. (2000). A new look at Syk in $\alpha\beta$ and $\gamma\delta$ T cell development using chimeric mice with a low competitive hematopoietic environment. J. Immunol. *164*, 5140–5145.

Dyson, N. (1998). The regulation of E2F by pRB-family proteins. Genes Dev. *12*, 2245–2262.

Fantl, V., Stamp, G., Andrews, A., Rosewell, I., and Dickson, C. (1995). Mice lacking cyclin D1 are small and show defects in eye and mammary gland development. Genes Dev. *9*, 2364–2372.

Harbour, J.W., Luo, R., Dei Santi, A., Postigo, A., and Dean, D. (1999). Cdk phosphorylation triggers sequential intramolecular interactions that progressively block Rb functions as cells move through G1. Cell *98*, 859–869.

Huard, J., Forster, C., Carter, M., Sicinski, P., and Ross, M. (1999). Cerebellar histogenesis is disturbed in mice lacking cyclin D2. Development *126*, 1927–1935.

Jacobs, J., Kieboom, K., Marino, S., DePinho, R., and van Lohuizen, M. (1999). The oncogene and Polycomb-group gene bmi-1 regulates

cell proliferation and senescence through the ink4a locus. Nature *397*, 164–168.

Kondo, M., Weissman, I., and Akashi, K. (1997). Identification of clonogenic common lymphoid progenitors in mouse bone marrow. Cell *91*, 661–672.

Lam, E., Glassford, J., Banerji, L., Thomas, N., Sicinski, P., and Klaus, G. (2000). Cyclin D3 compensates for loss of cyclin D2 in mouse B-lymphocytes activated via the antigen receptor and CD40. J. Biol. Chem. *275*, 3479–3484.

Lundberg, A., and Weinberg, R. (1998). Functional inactivation of the retinoblastoma protein requires sequential modification by at least two distinct cyclin-cdk complexes. Mol. Cell. Biol. *18*, 753–761.

Malumbres, M., Sotillo, R., Santamaría, D., Galán, D.J., Cerezo, A., Ortega, S., Dubus, P., and Barbacid, M. (2004). Mammalian cells cycle without the D-type cyclin-dependent kinases Cdk4 and Cdk6. Cell *118*, this issue, 493–504.

Matsushime, H., Roussel, M., Ashmun, R., and Sherr, C. (1991). Colony-stimulating factor 1 regulates novel cyclins during the G1 phase of the cell cycle. Cell *65*, 701–713.

Meyer, C., Jacobs, H., Datar, S., Du, W., Edgar, B., and Lehner, C. (2000). Drosophila Cdk4 is required for normal growth and is dispensable for cell cycle progression. EMBO J. *19*, 4533–4542.

Molofsky, A., Pardal, R., Iwashita, T., Park, I.K., Clarke, M., and Morrison, S. (2003). Bmi-1 dependence distinguishes neural stem cell self-renewal from progenitor proliferation. Nature *425*, 962–967.

Morrison, S., Hemmati, H., Wandycz, A., and Weissman, I. (1995). The purification and characterization of fetal liver hematopoietic stem cells. Proc. Natl. Acad. Sci. USA *92*, 10302–10306.

Motokura, T., Bloom, T., Kim, H., Juppner, H., Ruderman, J., Kronenberg, H., and Arnold, A. (1991). A novel cyclin encoded by a bcl1-linked candidate oncogene. Nature *350*, 512–515.

Ortega, S., Prieto, I., Odajima, J., Martin, A., Dubus, P., Sotillo, R., Barbero, J., Malumbres, M., and Barbacid, M. (2003). Cyclin-dependent kinase 2 is essential for meiosis but not for mitotic cell division in mice. Nat. Genet. *35*, 25–31.

Park, M., and Krause, M. (1999). Regulation of postembryonic G(1) cell cycle progression in Caenorhabditis elegans by a cyclin D/CDK-like complex. Development *126*, 4849–4860.

Park, I., Qian, D., Kiel, M., Becker, M., Pihalja, M., Weissman, I., Morrison, S., and Clarke, M. (2003). Bmi-1 is required for maintenance of adult self-renewing haematopoietic stem cells. Nature *423*, 302–305.

Perez-Roger, I., Kim, S., Griffiths, B., Sewing, A., and Land, H. (1999). Cyclins D1 and D2 mediate myc-induced proliferation via sequestration of p27(Kip1) and p21(Cip1). EMBO J. *18*, 5310–5320.

Rane, S., Dubus, P., Mettus, R., Galbreath, E., Boden, G., Reddy, E., and Barbacid, M. (1999). Loss of Cdk4 expression causes insulin-deficient diabetes and Cdk4 activation results in β-islet cell hyperplasia. Nat. Genet. *22*, 44–52.

Serrano, M., Gomez-Lahoz, E., De Pinho, R., Beach, D., and Bar-Sagi, D. (1995). Inhibition of ras-induced proliferation and cellular transformation by p16INK4. Science *267*, 249–252.

Sherr, C., and Roberts, J. (1999). CDK inhibitors: positive and negative regulators of G1-phase progression. Genes Dev. *13*, 1501–1512.

Sicinska, E., Aifantis, I., Le Cam, L., Swat, W., Borowski, C., Yu, Q., Ferrando, A., Levin, S., Geng, Y., von Boehmer, H., and Sicinski, P. (2003). Requirement for cyclin D3 in lymphocyte development and T cell leukemias. Cancer Cell *4*, 451–461.

Sicinski, P., Donaher, J., Parker, S., Li, T., Fazeli, A., Gardner, H., Haslam, S., Bronson, R., Elledge, S., and Weinberg, R. (1995). Cyclin D1 provides a link between development and oncogenesis in the retina and breast. Cell *82*, 621–630.

Sicinski, P., Donaher, J.L., Geng, Y., Parker, S.B., Gardner, H., Park, M.Y., Robker, R.L., Richards, J.S., McGinnis, L.K., Biggers, J.D., et al. (1996). Cyclin D2 is an FSH-responsive gene involved in gonadal cell proliferation and oncogenesis. Nature *384*, 470–474.

Solvason, N., Wu, W.W., Parry, D., Mahony, D., Lam, E.W., Glassford, J., Klaus, G.G., Sicinski, P., Weinberg, R., Liu, Y.J., et al. (2000). Cyclin D2 is essential for BCR-mediated proliferation and CD5 B cell development. Int. Immunol. *12*, 631–638.

Spangrude, G., and Scollay, R. (1990). Differentiation of hematopoietic stem cells in irradiated mouse thymic lobes. J. Immunol. *145*, 3661–3668.

Sucov, H. (1998). Molecular insights into cardiac development. Annu. Rev. Physiol. *60*, 287–308.

Traver, D., Miyamoto, T., Christensen, J., Iwasaki-Arai, J., Akashi, K., and Weissman, I. (2001). Fetal liver myelopoiesis occurs through distinct, prospectively isolatable progenitor subsets. Blood *98*, 627–635.

Tsutsui, T., Hesabi, B., Moons, D., Pandolfi, P., Hansel, K., Koff, A., and Kiyokawa, H. (1999). Targeted disruption of CDK4 delays cell cycle entry with enhanced p27(Kip1) activity. Mol. Cell. Biol. *19*, 7011–7019.

Weinstat-Saslow, D., Merino, M.J., Manrow, R., Lawrence, J., Bluth, R., Wittenbel, K., Simpson, J., Page, D., and Steeg, P. (1995). Overexpression of cyclin D mRNA distinguishes invasive and in situ breast carcinomas from non-malignant lesions. Nat. Med. *1*, 1257–1260.

Xiong, Y., Connolly, T., Futcher, B., and Beach, D. (1991). Human D-type cyclin. Cell *65*, 691–699.

Zarkowska, T., and Mittnacht, S. (1997). Differential phosphorylation of the retinoblastoma protein by G1/S cyclin-dependent kinases. J. Biol. Chem. *272*, 12738–12746.